Mon. Not. R. astr. Soc. (1992) **255**, 165–176

On warmers as the ionizing source in active galactic nuclei

R. Cid Fernandes Jr,[1,2] H. A. Dottori,[3] R. B. Gruenwald[1] and S. M. Viegas[1]

[1] *Instituto Astronômico e Geofísico, Universidade de São Paulo, Caixa Postal 9638, 01065 São Paulo, Brazil*
[2] *Institute of Astronomy, Madingley Road, Cambridge CB3 0HA*
[3] *Instituto de Física, Universidade Federal do Rio Grande do Sul, Caixa Postal 15051, 90069 Porto Alegre, Brazil*

Accepted 1991 October 3. Received 1991 September 30; in original form 1991 June 26

SUMMARY

The aim of this paper is to study in detail the Terlevich & Melnick starburst–warmers scenario for type 2 Seyferts and LINERs, which postulates a young cluster containing stars with temperatures about 150 000 K as the heating source in these objects. A numerical code was developed to compute the total spectrum of a star cluster given its age and initial mass function. The ionizing spectra so obtained were used in the photoionization code AANGABA to calculate the nebular emission-line spectra for a grid of cloud parameters covering different densities (and gradients), ionization parameters and metallicities. The evolution of the system was followed on classical diagnostic diagrams and a very good agreement with Terlevich & Melnick's results was found. We conclude that warmers can indeed be the ionizing source in many narrow-line AGN, although the coverage of AGN areas on diagnostic diagrams is not complete. We find the warmers model successful within a metallicity range between ≈ 0.5 and $2\,Z_{\odot}$. The upper limit is set by the strong cloud cooling by forbidden lines. On the other hand, at $Z \lesssim 0.5\ Z_{\odot}$ fewer stars would be thrown into 'warmer' phases due to the smaller mass-loss rates, and even if warmers occur the emission-line spectrum would correspond to an H II galaxy rather than to an AGN. The chemical pollution of the gas by the strongly processed stellar winds of massive stars is also studied. Our results suggest that the nitrogen overabundance of AGN frequently claimed in the literature arises quite naturally in this scenario.

1 INTRODUCTION

Historically, the concept of 'activity' arose from observations of galactic nuclei whose optical emision-line features could not be understood in terms of normal star-formation processes. Classification schemes were proposed to separate 'active' from 'normal' objects on the basis of optical line intensity ratios (Baldwin, Phillips & Terlevich 1981; Veilleux & Osterbrock 1987). The high-excitation objects (Seyferts and radio galaxies) and the low-excitation ones (LINERs) could be distinguished from H II-like objects by means of their positions on diagnostic diagrams. However, radio, infrared and X-ray surveys point to a continuity and/or overlap of properties rather than a fundamental dichotomy between these two classes (Condon *et al.* 1982; Lawrence *et al.* 1985; Rodriguez Espinosa, Rudy & Jones 1987; Armus, Heckman & Miley 1989; Forbes *et al.* 1991). In addition, several 'composite' objects, showing H II regions around an active galactic nucleus (AGN) or active 'spots' in a starburst region are now known (McCarthy, Heckman & van Breugel 1987; Heckman, Armus & Miley 1987; Kennicutt, Keel & Blaha 1989; Shields & Filippenko 1990). Phenomenologically, star formation and activity seem to be linked in some as yet undefined way.

The most popular attempts to explain such a connection explore the idea of the dynamical evolution of a star cluster collapsing to form a super-massive black hole (e.g. Weedman 1983; Rees 1984; Norman & Scoville 1988). In this scenario, the line-emitting gas is photoionized by high-energy photons produced in an accretion disc around the black hole – the so-called 'monster' paradigm. Photoionization models assuming a power law for the ionizing spectrum ($L_{\nu} \sim \nu^{-\alpha}$) could link Seyfert 2s and LINERs in a sequence of decreasing ionization parameter, U (Ferland & Netzer 1983; Halpern & Steiner 1983). A common drawback of these earlier models is that the best fit to classical AGN line ratios is obtained for under-solar chemical abundances, which is in conflict with other observational and theoretical evidence (e.g. Pagel & Edmunds 1981). Further improvements in photoionization models – such as considering the effects of clouds of different densities and optical thicknesses (Péquignot 1984; Viegas Aldrovandi & Gruenwald 1988, hereinafter VAG), ioniza-

tion parameters (Binette 1985), geometry (Ferland & Osterbrock 1986), ionizing spectrum (Binette, Robinson & Courvoisier 1988), or a flux of relativistic electrons (Gruenwald & Viegas Aldrovandi 1987) – lead to a reasonable fitting of the strong lines using solar metallicities. A general conclusion of all models is that the ionizing source should emit strongly in the UV to X-ray range, seeming to rule out young, hot stars as the energy source and discarding any resemblance to starburst models.

Terlevich & Melnick (1985, hereinafter TM) brought new breath to the starburst hypothesis for AGN. Using the evolutionary tracks of Maeder & Meynet (1987), they computed the evolution of the ionizing spectrum of a young star cluster, which was then used as an input to the photoionization code CLOUDY (Ferland & Truran 1981). Their main point was that after about 3 Myr the most massive stars reverse their redward track in the HR diagram, reaching effective temperatures ($T_{\rm eff}$) as high as 150 000 K ('warmers') as a result of the continuous removal of the outer layers by strong mass loss. Such large values of $T_{\rm eff}$ provide the high-energy photons that are needed to ionize active nuclei, but are absent in standard H II regions. They have shown that such a system evolves from an initial normal phase (H II region) to an active one (Seyfert 2 and/or LINER) on diagnostic diagrams. Thus, as they have claimed, the mere existence of warmers could represent 'the missing link between starburst and Seyfert galaxies'. Terlevich and collaborators further extended this model by including the effects of supernova events (explosion and remnants), which could account for the observed properties of the broad-line region (BLR) of type 1 Seyferts and QSOs (Terlevich, Melnick & Moles 1987; Terlevich *et al.* 1991a; Filippenko 1989a).

In recent years, the opinion has grown that AGN may indeed constitute a rather heterogeneous class of objects, comprising distinct physical situations ('monsters', starbursts, shock waves, mergers, starburst-driven winds, composite objects), as pointed out by Heckman (1987), McCarthy *et al.* (1987), Filippenko (1989a), Viegas Aldrovandi & Contini (1989), Viegas Aldrovandi & Gruenwald (1990) and Heckman *et al.* (1990). In fact, much attention has been devoted to the possible links between star formation and activity. Nevertheless, no independent assessment of the extreme theory of this link – the idea that AGN *are* a manifestation of starburst activity, as claimed by Terlevich and collaborators – has been carried out [see, however, the criticism by Heckman (1991)].

It is our purpose in this paper to investigate in detail the starburst–warmers model for Narrow-Line AGN in order to verify which objects can be reasonably explained in this way. First (Section 2) we review what is currently known about the key point of this model, namely, the existence of warmers. In Section 3 we describe the 'synthesis' code developed to calculate the spectrum of an ionizing cluster given its age and initial mass function (IMF). A grid of photoionization models was then built using the code AANGABA (Gruenwald & Viegas 1992), varying the cluster age (t), ionization parameter (U), cloud density (n) and metallicity (Z). These results are presented and discussed in Section 4. In Section 5 we address a very interesting question not discussed by TM: the chemical pollution of AGN clouds by the metal-rich winds of Wolf-Rayet (WR) stars and warmers. From Maeder & Meynet (1988, hereinafter MM) and the new Maeder (1990) tables we compute the changes in the wind abundances and, with a simple model, verify how the enrichment of the surrounding gas alters the final emission lines. Special attention is devoted to the case of nitrogen, in view of its possible overabundance claimed in recent works (Binette 1985; Storchi Bergmann & Pastoriza 1989, 1991). Finally in Section 6 we summarize our results and draw our conclusions.

2 WARMERS

2.1 Do warmers exist at all?

From the very first evolutionary calculations including mass loss it was found that stars above a certain initial mass go through an extremely hot and luminous phase near the He zero-age main sequence (ZAMS). This is a common trend in virtually all models (Tanaka 1966; de Loore 1982; Bertelli, Bressan & Chiosi 1984; Sreenivasan & Wilson 1985; Doom 1985; MM; Maeder 1990), the details depending strongly on the mass loss and, to a lesser degree, overshooting parametrizations adopted (Chiosi & Maeder 1986). Because of the resulting surface abundances, these hot (over 100 000 K) stages are usually associated with WR stars, although WR temperatures reported in the literature range from 25 000 to 60 000 K in most cases. These values, however, must not be directly compared, since there are several uncertainties in modelling the complex atmospheres of WR stars. In any case, it is generally agreed that the dense winds of these stars might decrease the surface temperature (given by the evolutionary models) and alter the output spectra as a whole (Langer *et al.* 1988; Langer 1989).

There is, nevertheless, convincing evidence that at least some WR stars may be much hotter than commonly believed. Davidson & Kinman (1982) reported the presence of an extreme WO star ionizing an H II region in a nearby galaxy (IC 1613). The H II-region spectrum indicates a Zanstra temperature of 110 000 K for the ionizing radiation. Barlow & Hummer (1982) characterized the WO sequence as extremely hot WR stars, fitting effective temperatures between 150 000 and 200 000 K to their optical–UV data. Perhaps the most convincing example of such a hot star comes from the Dopita *et al.* (1990) analysis of the emission-line spectrum of the G2.4 + 1.4 nebula photoionized by the WO star WR 102. They could not fit the nebular spectroscopic characteristics for ionization temperatures below 150 000 K! The strength of nebular He II λ4686-Å emission provides a good measure of the hardness of the radiation field in photoionized nebulae. Several independent studies exploring this line have shown that WR stars (especially WOs, but also some early WNs) may be much hotter than normal OB stars, which are not hot enough to doubly ionize helium significantly (Melnick & Heydari Malayeri 1991; Garnett *et al.* 1991; Pakull 1991; Pakull & Bianchi 1991). Temperatures in the 70 000–100 000 K range are quoted in these works. Detailed modelling of the ionization structure of ring nebulae support these high values for $T_{\rm eff}$ (Rosa & Mattews 1990). Some of the most metal-poor H II galaxies in Melnick & Terlevich (1987) also seem to require ionization temperatures in excess of 100 000 K (see also Johansson, Westerlund & Azzopardi 1990).

Theoretically, it is still unclear how hot these extreme WR stars may really be, but the fact that these observations indicate very high temperatures shows that not all ionizing photons are trapped within their envelopes and that these

stars may indeed be powerful sources of ionization. It is, in any case, relevant to point out that these stars are obviously expected to be rarely found due both to their short life and their high bolometric correction (most of their light is emitted in UV–X-ray bands). Furthermore, very little is known about the evolution of massive stars under the high-metallicity conditions expected in the nuclei of early-type spirals (where most AGN occur). It is certainly not the case that *all* WR stars are so hot, but the above reviewed works put the existence of warmers on good observational grounds, and a second and independent assessment of this alternative model for AGN is desirable.

In Fig. 1 we plot the time evolution of $T_{\rm eff}$ for the most massive MM models. There we can see that stars spend an appreciable time (typically 0.5 Myr) in the 140 000–160 000 K range, almost independent of the initial mass, undertaking brief temperature variations at the end of C burning (pre-supernova stage). Note the occurrence of red supergiant (RSG) stages prior to the rapid WR/warmer onset, which happens only for stars with initial mass within ≈ 30 to 50 $M_{\odot}$. As we shall see later, this may have important observational consequences.

Recently, a new set of massive stellar evolutionary tracks for four different metallicities ($Z = 0.1$, 0.25, 1 and $2\,Z_{\odot}$) has been published by Maeder (1990). In these models the effective temperatures of WR phases have been corrected by the rough method outlined by de Loore, Hellings & Lamers (1982) and Langer (1989). It turns out to yield $T_{\rm eff}$ up to a maximum of about 120 000 K, lasting for only some 10^4 yr. Also, there is no plateau in $T_{\rm eff}$ during the post-main-sequence evolution as in MM, due to the different treatment of $\dot{M}$. The models adopt a $\dot{M} \propto M_{\rm WR}^{2.5}$ (where $M_{\rm WR}$ is the current mass of WR stages) parametrization for the mass-loss rate during WR phases, which results in much stronger mass losses, thus smaller WR masses and luminosities. Although the main calculations were performed with MM tracks, an investigation of the changes introduced by these new tables is discussed in subsequent sections.

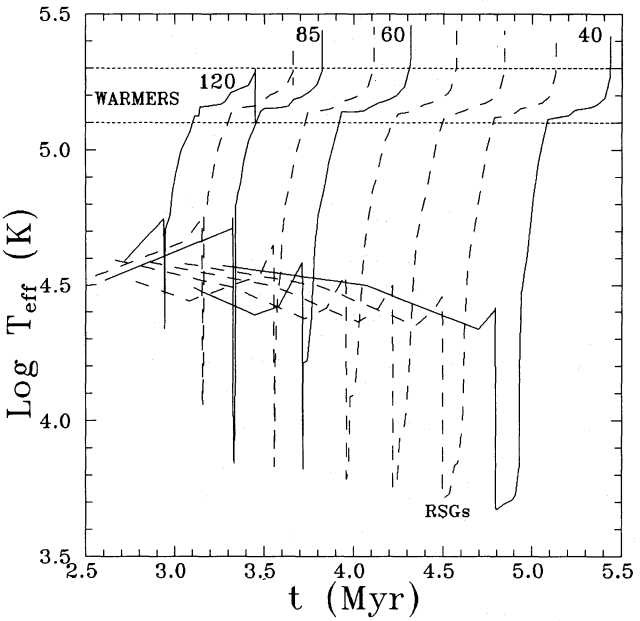

Figure 1. Evolution of the effective temperature for the most massive stars in MM. Numbers beside each solid line indicate the initial mass in $M_{\odot}$. Dashed lines are interpolated tracks for 100, 70, 55, 50 and 45 $M_{\odot}$.

2.2 The role of the metallicity

In the theory of radiatively driven winds, mass-loss rates are expected to grow with metal content (Z), because greater opacities increase the efficiency of line acceleration by radiation pressure (e.g. Castor, Abbott & Klein 1975). Abbott (1982) has proposed $\dot{M} \propto Z$ and Kudritsky, Pauldrach & Puls (1987) $\dot{M} \propto Z^{0.47}$ for O and B stars (pre-WRs), the latter having stronger observational support (Leitherer 1988; Azzopardi, Lequeux & Maeder 1988). However, evolutionary calculations make use of semi-empirical parametrizations for $\dot{M}$ instead of adopting such theoretical prescriptions. MM, for example, use the parametrization for $\dot{M}$ found for stars in the solar vicinity (de Jager, Nieuwenhuijzen & van der Hucht 1988), with $Z \approx Z_{\odot}$. Maeder (1990) adopts a $(Z/Z_{\odot})^{0.5}$ scaling for $\dot{M}/\dot{M}(Z_{\odot})$ (during pre-WR phases), $\dot{M}(Z_{\odot})$ being calculated in the same MM semi-empirical way. A fully consistent picture of these stars, incorporating theoretical mass-loss rates and an adequate description of the windy envelope, is yet to be achieved.

By affecting $\dot{M}$, the metallicity has decisive effects on the evolution of massive stars. The higher Z is, the higher $\dot{M}$ and, therefore, the smaller the minimum initial mass for a star to become a WR ($M_{\rm WR}^{\rm min}$). The exact WR subtype evolution may also be affected by Z. Maeder (1991) finds that early WCE and WO stages have comparatively longer lifetimes in metal-poor environments. The actual number of WRs (of all subtypes), however, will be bigger the higher Z is (due to the lower initial masses required), and we expect the occurrence of warmers (understood as extreme WOs and/or WCEs) to be favoured in metal-rich regions (unless IMF changes with Z are invoked). They may, nevertheless, occur in metal-poor regions as well, in accordance with the few known cases, (Melnick & Heydari Malayeri 1991). On Maeder's (1990) tracks $M_{\rm WR}^{\rm min}$ decreases from ≈ 65 to 22 $M_{\odot}$ for Z increasing from 0.1 to $2\,Z_{\odot}$. In MM models ($Z = Z_{\odot}$) $M_{\rm WR}^{\rm min}$ lies somewhere between 25 and 40 $M_{\odot}$.

2.3 Metal-rich starbursts

The above discussion on the metallicity role has important consequences for the interpretation of starbursts at high Z. It is clear that high-Z star-forming regions will naturally favour WR/warmers' occurrence. Statistical studies of the ratio between the number of WR and OB stars in Local Group galaxies do confirm the theoretically expected trend with metal content, metal-rich media being more efficient in WR production (Maeder, Lequeux & Azzopardi 1980; Smith 1988; Azzopardi *et al.* 1988). This raises the question of metallicities in galactic nuclei. For AGN, several lines of evidence indicate abundances in the 1–$2\,Z_{\odot}$ range (Evans & Dopita 1987; Bonatto, Bica & Alloin 1989; Storchi Bergmann & Pastoriza 1989). For H II nuclei, Terlevich *et al.* (1991b) report a remarkable lack of metal-rich H II galaxies in a survey of about 450 objects, most of them having under-solar abundances. Other studies confirm this fact (Campbell 1988). The starburst–warmers scenario provides a natural interpretation for this dichotomy, since the metal poorness

of H II galaxies makes them inappropriate ambient media for a warmers 'culture'. In other words, metal-rich starbursts would look like AGN! Furthermore, as we shall see, even when warmers occur in low-metallicity systems they do not produce AGN-like line ratios; instead, a H II-region-type spectrum would result (Section 4.4).

Besides the Z role, the abundant molecular gas observed in AGN can fuel massive bursts of star formation (Heckman *et al.* 1989; Solomon, Radford & Downes 1990). Dust (Sanders *et al.* 1988), young stars (Terlevich, Díaz & Terlevich 1990; Jarvis & Melnick 1991) and other ingredients common to star-forming regions are also observed. This, together with the high metallicities, makes AGN ideal loci for the occurrence of warmers.

3 THE IONIZING SPECTRUM

3.1 The 'synthesis' code

To obtain the total spectrum of a theoretical star cluster one needs: (i) a set of evolutionary tracks; (ii) an IMF [$\phi(M)$], and (iii) model atmospheres. We developed a computer code – which will be referred to as 'ET', acronym for 'Total Spectrum' in Portuguese – which calculates the spectrum of each star (F_ν^*) from a 2D interpolation of model atmosphere spectra in the $\log g - T_{\rm eff}$ plane, then sums up the contribution of each star, properly weighted by an IMF, to the total luminosity at a frequency ν according to

$$L_\nu(t, IMF) = \int_{M_{\rm low}}^{M_{\rm up}} 4\pi R_*^2 F_\nu^* \phi(M)\, dM, \qquad (1)$$

where M, R_* and F_ν^* are the stellar (initial) mass, radius and spectral flux at age t. $M_{\rm low}$ and $M_{\rm up}$ are the lower and upper IMF mass limits. For the spectrum in the 0.1–416 eV range, 240 frequency bins were used.

The stellar evolutionary tracks used are the MM ones. The IMF was taken as $\phi(M) \propto M^{-(1+\chi)}$ (Salpeter 1955). The normalization constant is linearly proportional to the total cluster mass ($M_{\rm T}$), i.e., to the mass of gas converted into stars in the burst, which was supposed to be instantaneous, as suggested by several studies of violent star-formation processes (Dottori & Bica 1981; Lequeux *et al.* 1981; Melnick, Terlevich & Eggleton 1985; Copetti, Pastoriza & Dottori 1986). The adopted mass limits are $M_{\rm up} = 120$ and $M_{\rm low} = 3\,M_\odot$. Stars less massive than $3\,M_\odot$ have contraction time-scales greater than 1 Myr, and, apart from taking longer to form, their formation may be inhibited by the destructive effects of early supernovae and winds from the upper IMF stars. This is consistent with observations of the well-studied starburst region, 30 Dor, where no stars below $\approx 4\,M_\odot$ are seen (Melnick 1987). In any case, $M_{\rm low}$ clearly does not affect photoionization calculations since low-mass stars do not significantly contribute to the UV emission, but its value strongly changes $M_{\rm T}$, which, as we will see, is directly related to the ionization parameter U.

Model atmospheres were taken from Kurucz (1979) for stars in the 5500–50 000 K range, Clegg & Middlemass (1987) for the 50 000–70 000 K range and Wesemael (1981) pure He models for $T_{\rm eff} > 70\,000$ K. Pure He is indeed a reasonable approximation to warmers, as can be seen from the surface abundances in the MM tables. The critical point here is the use of standard static, plane-parallel, Local Thermodynamic Equilibrium (LTE) models for the windy, extended, non-LTE envelopes of warmers. This becomes evident when we follow the evolution of the most massive stars in the $\log g - T_{\rm eff}$ plane, where they evolve very close to the Eddington limit, below the lower $\log g$ Wesemael models – in these cases interpolations were performed only in $T_{\rm eff}$. This problem illustrates the need (stressed in Section 2.1) for better WR/warmer model atmospheres.

3.2 Evolution

The evolution of the ionizing spectrum (normalized to $M_{\rm T} = 1\,M_\odot$) is plotted in Fig. 2 with the resulting simulated optical emission-line spectra (for a particular set of cloud parameters) which will be discussed in Section 4. The ages were chosen in order to emphasize the drastic changes when warmers are produced in the ionizing cluster.

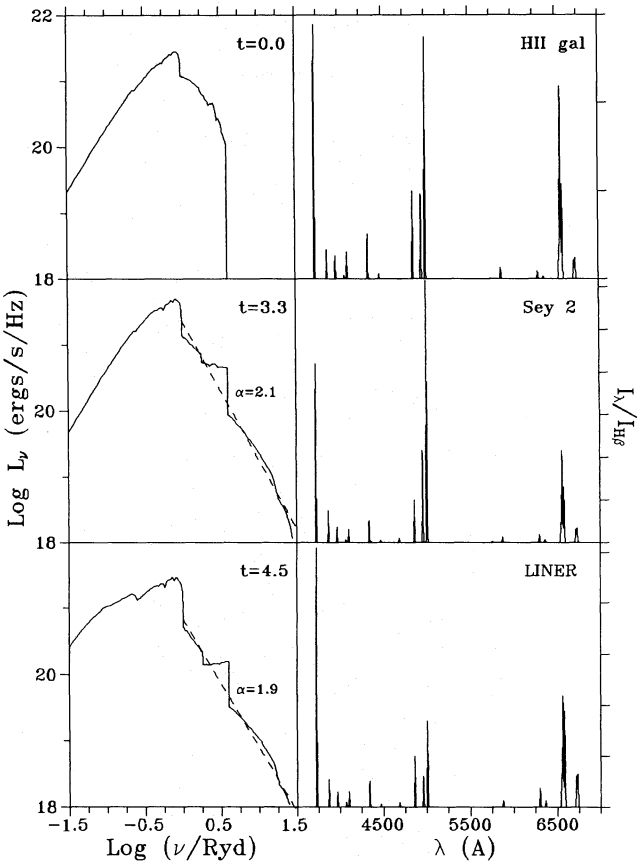

Figure 2. Evolution of the spectral energy distribution of the ionizing cluster (left) and the corresponding nebular emission lines (right). L_ν is normalized to $M_{\rm T} = 1\,M_\odot$. The top right labels in each figure are the age in Myr and the spectral type of the emitting nucleus. Dashed lines for $t = 3.3$- and 4.5-Myr spectra show the fitted power laws. The emission-line spectra correspond to a $Z = Z_\odot$, $U_{\rm max} = 10^{-3}$ and $n = 10^3$ cm^{-3} model sequence. [O II] 3726, 3729; [Ne III] 3868, 3967; Hε 3970; [S II] 4070, 4077; Hδ 4101; Hγ 4340; [O III] 4363; He II 4686; Hβ 4861; [O III] 4959, 5007; [N II] 5755; He I 5876; [O I] 6300, 6363; [N II] 6548, 6584; Hα 6563, and [S II] 6717, 6731 Å lines have been included in the plot. Ticks in the intensity scale are multiples of Hβ intensity.

H II phase. At age 0 the UV spectrum is dominated by O and B ZAMS stars and is typical of a high ionizing temperature H II region.

Active phase. At 3.3 Myr, the UV emission increases drastically and extends to higher energies due to the high-$T_{\rm eff}$ photons emerging from the first warmers. At 4.5 Myr this high-energy emission is weaker, since stars with initial masses $\gtrsim 55\,M_\odot$ have already 'died' as faint (type Ib?) supernovae. The infrared (IR) region, instead, grows strongly due to the presence of RSGs in the cluster (see Fig. 1).

After $t \approx 6$ Myr all massive stars have evolved and a weak 'inactive' source remains. If the burst is not instantaneous but instead lasts for some Myr, these time-scales are expected to change; the qualitative evolutionary picture, however, would remain valid.

A key result (as in TM) is that the overall shape of the high-energy spectrum in the active phase closely resembles a power law. Indeed, fitting a $L_\nu \propto \nu^{-\alpha}$ curve to the spectrum above 13.6 eV yields $\alpha = 2.1$ for 3.3 Myr and 1.9 for 4.5 Myr (dashed lines in Fig. 2), with small residuals. Varying the IMF slope, χ, affects the fitted power-law index: for a 3.3-Myr cluster α ranges from 1.9 to 2.3 for χ between 0.5 and 2.5 respectively, while for a 4.5-Myr cluster it varies from 1.8 to 2.0 for the same χ values. Most photoionization models for Seyfert 2s and LINERs use this kind of ionizing spectrum with $\alpha \approx 1$–2 (Ferland & Netzer 1983; Binette 1985; Ferland & Osterbrock 1986; VAG). Thus, from our fitted values of α, we expect photoionized clouds to have AGN-like emission-line spectra prior to any photoionization calculations – which is indeed confirmed in the emission-line spectra shown in Fig. 2 and the subsequent analysis in Section 4. Here, however, this shape is a natural consequence of the cluster evolution rather than an ad hoc assumption. The α range we found is in perfect agreement with $\alpha \approx 2 \pm 0.2$, proposed by Binnette (1985) in his LINER models. It is, however, steeper than most models for type 2 Seyferts: $\alpha = 1.5$ (Ferland & Osterbrock 1986) and $\alpha = 1.0$ (Ferland & Netzer 1983). Indeed, the mean energy of ionizing photons during the active phase is $\varepsilon \approx 30 \pm 2$ eV, in marginal agreement with the 30–40 eV range quoted by Binette *et al.* (1988). The relative number of warmers to OB stars determines the slope of the ionizing spectrum. Experiments changing this ratio by factors of about 2 showed that the ionizing continuum can easily get as flat as $\alpha = 1.5$. Such enhancement of WR/warmers over OB stars actually occurs in the new Maeder (1990) 2-$Z_\odot$ models. It seems that there is still room within the models to find harder ionizing fluxes (lower values of α), although a more detailed analysis will be necessary to check how critical this may be.

The near-IR enhancement from 4.5 Myr on (Fig. 2) is due to the RSGs occurring prior to WR/warmer phases (Fig. 1). Such stars were indeed detected in AGN through the measurement of the Ca II 8498, 8542, 8662-Å absorption triplet (Terlevich *et al.* 1990; Jarvis & Melnick 1991). Furthermore, these lines are not diluted with respect to normal galaxies, contrary to what is expected in the power-law 'model' for the continuum in AGN. A young stellar population, on the other hand, can produce a blue and featureless continuum and still have the Ca II lines in the appropriate strength (Kinman & Davidson 1981; Cid Fernandes & Terlevich 1991).

A useful quantity to study the cluster evolution is the ionizing photon emission rate $Q_{\rm H}$, which, in this scenario, depends on cluster age and IMF. Since $\phi(M) \propto M_{\rm T}$, the $Q_{\rm H}$ dependence on the burst mass can be separated from the evolutionary and IMF-shape effects by writing $Q_{\rm H}(t, IMF) = q_{\rm H}(t, \chi)\, M_{\rm T}/M_\odot$. In Fig. 3 we plot the evolution of $q_{\rm H}(t, \chi)$ for various values of χ. During the H II phase it declines very slowly (as the most massive stars leave the ZAMS), rising again with the onset of the first warmers and then decaying steadily as the ionizing sources (OB stars and warmers) die. For a given age and χ, $M_{\rm T}$ can be estimated from the resulting Hα output luminosity using $L_{\rm H\alpha} \approx 1.38 \times 10^{-12} (Q_{\rm H}/s)$ ergs s^{-1}. If we take the strongest Seyfert 2s, $L_{\rm H\alpha} \approx 10^{43}$ ergs s^{-1}, to be in the peak of the active phase (3.3 Myr) and the weakest LINERs, $L_{\rm H\alpha} \approx 10^{38}$ ergs s^{-1}, to be on its minimum (5.5 Myr), $M_{\rm T}$ would be $\approx 5 \times 10^7$ and $3 \times 10^3\, M_\odot$ respectively (for $\chi = 1.35$). These limits are, however, rough approximations, since the adoption of other values for χ and $M_{\rm low}$ can easily change them by an order of magnitude.

The supernova (SNe) rate remains approximately constant around 2×10^{-9} SNe per year per unit $M_{\rm T}/M_\odot$ (for $\chi = 1.35$) during the active phase. The above limits on $M_{\rm T}$ give rates from 10^{-1} to 6×10^{-6} SNe per year from the strongest Seyfert 2 to the weakest LINER. SNe with WR/warmer progenitors are expected to be optically dimmer than those with RSG progenitors (type II), which are expected to occur later in the cluster evolution – and possibly cause the observed variability of the broad lines of type 1 Seyferts and QSOs (Terlevich *et al.* 1991a). Perhaps these faint SNe are type Ib; see Porter & Filippenko (1987) for a review of observational properties, and Ensman & Woosley (1988) for a recent model. [On the other hand, the observed properties of type Ib SNe suggest that most of them do *not* arise from WR stars; see Filippenko (1991), and Branch, Nomoto & Filippenko (1991).] SNe explosions and evolution of remnants will not be discussed here, but are indeed a promising vein of the starburst model to be explored in view of the 'Seyfert-like' spectra of SNe 1987F and 1988I (Filippenko 1989a, b).

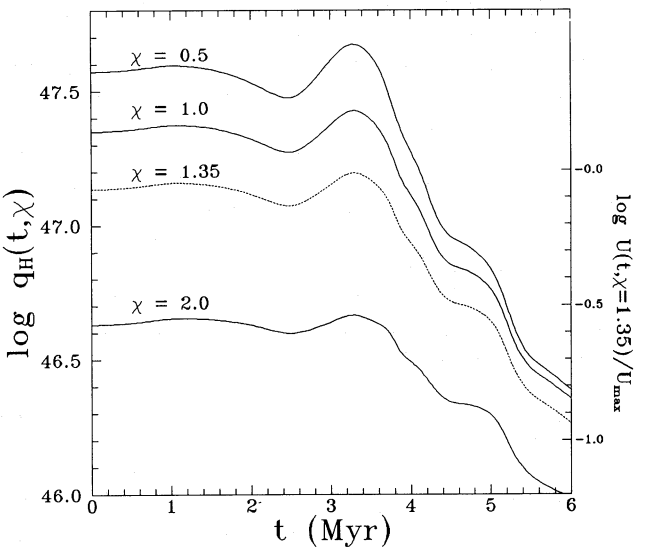

Figure 3. Evolution of the ionizing photon emission rate per unit $M_{\rm T}/M_\odot$. Each curve corresponds to the labelled IMF slope (χ). The right axis shows $\log[U(t, \chi)/U_{\rm max}]$ for $\chi = 1.35$.

4 PHOTOIONIZATION MODELS

4.1 The models

The ionizing spectra obtained with the code ET were used as an input to the photoionization code AANGABA (Gruenwald & Viegas 1992) to calculate the emission-line spectra. The cloud input parameters are the hydrogen density (n) and chemical abundances. Single-density models with $\log n$ (cm^{-3}) = 2, 3, 4, 5, 6 and 7 were computed and then used to calculate integrated models as in VAG. Cloud densities are assumed to vary with r^{-2} so that U remains the same for all clouds. A power-law distribution function for the density is assumed, i.e., $f(n) \propto n^{-\beta}$, with β in the range 0–3 (VAG). The integrated flux of a line λ is given by:

$$F_\lambda^{\mathrm{TOT}} = \int_{n_{\min}}^{n_{\max}} F_\lambda(n)\, f(n)\, dn, \qquad (2)$$

where $n_{\min}$ and $n_{\max}$ are 10^2 and 10^6 cm^{-3} respectively; $F_\lambda(n)$ is the single-density model flux of line λ. The integrations were performed with 40 bins, interpolating $F_\lambda(n)$ from single-density fluxes; $\beta = 0$ stands for the case of an equal number of clouds of all densities between $n_{\min}$ and $n_{\max}$, while $\beta = 3$ simulates a great predominance of low-density clouds. (Gaussian distribution profiles were also tested, but will be only briefly discussed below.) Such models try to account for the observational evidence of the presence of clouds with different densities in AGN (Filippenko & Halpern 1984; Filippenko & Sargent 1988).

In a starburst scenario the ionization parameter, $U \equiv Q_{\mathrm{H}}/4\pi cr^2 n$, evolves according to $Q_{\mathrm{H}}(t, IMF)$, being consequently proportional to the cluster mass M_{T}. (In all subsequent photoionization calculations an IMF slope $\chi = 1.35$ has been used.) Once U is chosen for a given cluster age, its evolution is entirely determined by the evolution of q_{H}. Since the ionizing continuum does not change significantly in shape during the active phase we expect changes in emission-line ratios to rely essentially upon the evolution of U. We refer to a temporal sequence of models by its ionization parameter at 3.3 Myr, $U_{\max}$, such that $U(t) = U_{\max} q_{\mathrm{H}}(t)/q_{\mathrm{H}}(3.3)$. (Fig. 3 shows $U(t)/U_{\max}$ for $\chi = 1.35$ in the right ordinate axis.)

The values for solar abundances (up to Fe) were taken from Grevesse & Anders (1989). Models were computed for $Z = 0.1$, 0.5, 1, 2 and $3\,Z_\odot$. (Stellar evolutionary tracks, however, are the MM $Z_\odot$ ones, whatever the cloud metallicity used. This inconsistency may have important consequences – like over/underestimating the number of warmers and consequently the hardness of the ionizing continuum – in view of the discussions in Sections 2 and 3.)

Five cluster ages were chosen to study the system evolution: 0, 2.5, 3.3, 4.5 and 5.5 Myr. The corresponding cluster evolutionary states are:

(i) Age Zero – ZAMS; most massive stars with $T_{\mathrm{eff}} \approx 54\,000$ K;

(ii) 2.5 Myr – the most massive stars have left the ZAMS on their red loop preceding the warmer stage, making the ionizing spectra energetically weaker; hottest stars with $T_{\mathrm{eff}} \approx 36\,000$ K;

(iii) 3.3 Myr – onset of the first warmers; beginning of the active phase;

(iv) 4.5 Myr – ionizing sources continuously 'dying' decreased UV emission; occurrence of RSGs, and

(v) 5.5 Myr – very few warmers and OB stars survive up to this age.

Clouds were assumed to be radiation-bounded and calculations were stopped when $\mathrm{H}^+/\mathrm{H} < 1$ per cent.

4.2 Results

The transition of the emission-line spectrum from an initial normal (H II) to an active (Seyfert 2 and/or LINER) phase in classical diagnostic diagrams by the time the first warmers appear is in excellent agreement with TM's results, and we refer to their paper for a description of the evolutionary aspects. Briefly, the whole system begins as an H II galaxy; at 2.5 Myr the softer ionizing spectrum (due to the lower values of T_{eff}) results in a low-excitation H II-like spectrum. Then, if $\log U_{\max} \gtrsim -3.4$, the onset of warmers at 3.3 Myr ignites the Seyfert 2 phase, which evolves into a LINER as the ionizing cluster fades. For lower $U_{\max}$ the Seyfert 2 step is skipped and the nucleus evolves from an H II galaxy directly to a LINER. The emission-line spectrum evolution illustrated in Fig. 2 corresponds to models with $\log U_{\max} = -3$, (i.e., $\log U = -3.1$, -3 and -3.5 for $t = 0$, 3.3 and 4.5 Myr respectively, according to the right-axis scale on Fig. 3), $n = 10^3$ cm^{-3} and $Z = Z_\odot$. The lines have been widened using Gaussian profiles with a FWHM of 500 km s^{-1}.

Instead of emphasizing the evolutionary aspects, we concentrate on the effects of varying model parameters to have a clearer picture of the scope of the warmers model (as far as optical emission lines are concerned). Within the classical analysis approach, this consists of comparing the theoretically defined areas with the observed characteristic loci of AGN and H II-like objects on diagnostic diagrams. In Figs 4–6 we draw diagnostic diagrams involving some important line ratios. The [N II]/Hα ratio, besides its classical importance, was chosen because of our particular interest in the nitrogen abundance problem. The [O I]/[O III] ratio is especially important because of its sensitivity to the hardness of the ionizing spectrum, the most common distinguishing property of H II regions from AGN. Finally, the [O II]/[O III] line ratio was plotted because it is very often used as a classification criterion to separate Seyfert 2s from LINERs. The conclusions we draw here were nevertheless based on inspection of several other diagrams as well. The fundamental parameters in these figures are U, β and Z – as mentioned above, the cluster age affects essentially the ionization parameter. For each value of U a family of integrated models for different values of β is plotted. The direction of increasing β is indicated by arrows, points corresponding to $\beta = 0$, 1.5 and 3. Solid, small and long dashed lines correspond to $Z = 1$, 0.5 and $2\,Z_\odot$ respectively. U decreases downwards in all diagrams. Models with $\beta = 0$ and 3 and different ionization parameters were linked by dotted lines (ticks corresponding to $\log U = -2.5$, -3, -3.5 and -4), defining a theoretical area on these diagrams for each value of Z (except in Fig. 4, where areas were not drawn for the sake of clarity). Single-density models with $n = 10^4$ cm^{-3} are also plotted in Fig. 4 for $[\mathrm{N/H}] = 1$, 2 and 5 $[\mathrm{N/H}]_\odot$ (keeping solar abundances for all other elements) for the purpose of comparison. The data for Seyfert 2s (squares) and LINERs (triangles) plotted in these diagrams were kindly

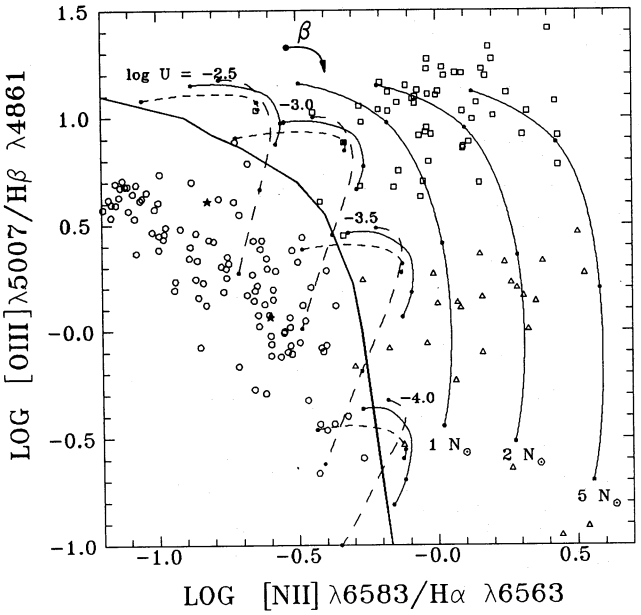

Figure 4. Integrated photoionization models. Open symbols are observed line ratios for Seyfert 2s (squares), LINERs (triangles) and H II galaxies (circles). The heavy line draws the 'borderline' between H II and active objects (from Veilleux & Osterbrock 1987). The four sets of curves are labelled by the corresponding value of log U. Solid, small and long dashed lines correspond to $Z=1$, 0.5 and $2\,Z_{\odot}$ models for different values of β (points are plotted for $\beta=0$, 1.5 and 3). The arrow shows the direction of increasing β. Curves labelled 1, 2 and 5 $N_{\odot}$ are $n=10^4$ cm^{-3} homogeneous models with enhanced nitrogen. The two filled stars in the H II galaxies' region correspond to two homogeneous $Z=0.1\,Z_{\odot}$ models for the cluster in the active phase (see Section 4.4).

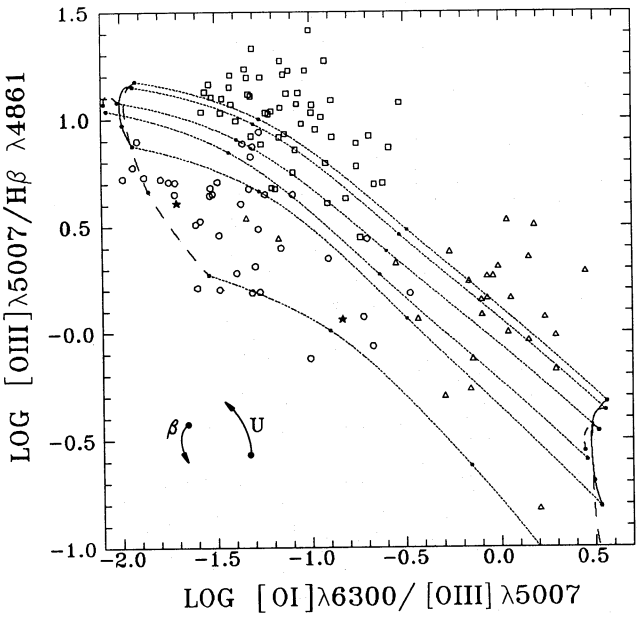

Figure 5. Same as Fig. 4 but for [O I] 6300/[O III] 5007 in the abscissa. Here the points with $\beta=0$ and 3 and same Z but different values of U have been linked with dotted lines, so that each set of models of a given Z defines an area in this diagram. The directions of increasing U and β are indicated (points correspond to the same values as in Fig. 4).

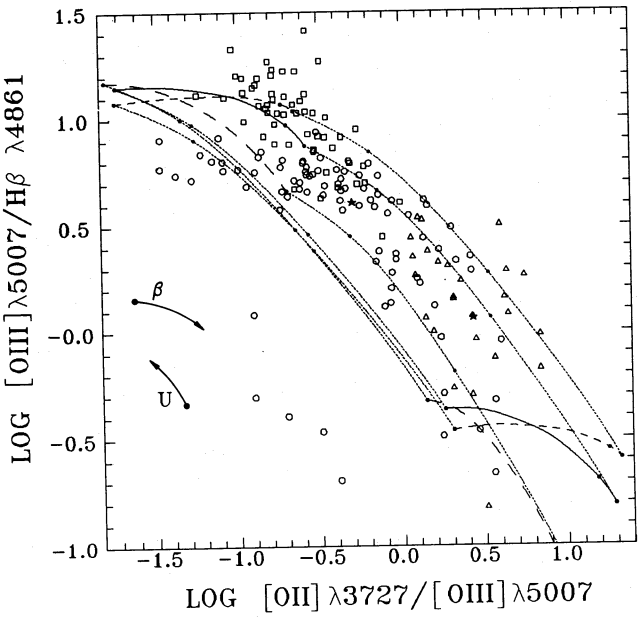

Figure 6. Same as Figs 4 and 5 but for [O I] 3727/[O III] 5007 in the abscissa. Models with $\beta=0$ and $2\,Z_{\odot}$ have not been plotted to avoid confusion, so that the $2\text{-}Z_{\odot}$ sequence ends in $\beta=1.5$ instead of 0 as for other values of Z.

made available by Dr T. Storchi Bergmann (for references see her 1991 paper). Line ratios for H II galaxies (circles) were taken from Terlevich *et al.* (1991b). In Fig. 4, the borderline dividing active and H II objects (long dashes) is from Veilleux & Osterbrock (1987).

Single-density models with n in the 10^3- to 10^4-cm^{-3} range give the best fit to AGN-like line ratios, in accordance with previous models (e.g. Ferland & Netzer 1983). Summing up the contributions of other clouds will, of course, worsen these single-density results (Fig. 4). This is most clearly seen in low-critical-density forbidden lines, like [O II] 3726, 3729 ($n_{\rm crit}=1.6\times10^4$ and 3.1×10^3 cm^{-3}), [S II] 6717, 6731 ($n_{\rm crit}=2\times10^3$ and 4×10^3 cm^{-3}) and [N II] 6583 ($n_{\rm crit}=8.6\times10^4$ cm^{-3}) for which lower values of β (i.e., greater contributions from dense, inner clouds) result in weaker lines. This illustrates the known fact that abundance determinations from single-density calculations tend to be underestimated if the observed spectra bear the contribution of a wide range of cloud densities (Péquignot 1984; Veilleux & Osterbrock 1987; VAG; Campbell 1990). The [O I] 6300 line ($n_{\rm crit}=2\times10^6$ cm^{-3}) shows the opposite behaviour with β, being more copiously produced in denser, hotter (see below) clouds (Fig. 5). The use of Gaussian distribution functions can favour $n=10^3$, 10^4 cm^{-3} models, provided adequate parameters are chosen. However, besides sounding more artificial, this is essentially equivalent to single-density calculations. (The $n=10^7$ cm^{-3} models computed were not included in line flux integrations; they strongly decrease the total emission of low-$n_{\rm crit}$ lines for β near 0, moving these models towards completely empty areas in diagnostic diagrams.)

The best-suited values for β turned out to depend on the metallicity: $\beta>1$ for $0.5<Z/Z_{\odot}<1$ (that is, a predominance of low-density clouds), whereas $\beta<1.5$ for $2\text{-}Z_{\odot}$ models. This is due to the well-known inverse correlation between Z and

the electronic temperature, T_e, in photoionized clouds (e.g., Péquignot 1984). Since higher Z results in lower T_e, hotter components must be invoked in order to keep the line intensities similar to those of lower Z models. Inner denser clouds may properly play this role, since the higher collisional de-excitation rates reduce radiative energy losses, consequently increasing the electronic temperature. An inevitable counterpart of low values of β is the weakness of low n_{crit} lines, especially [S II]6717, 6731 and [O II]3726, 3729.

An apparent problem of virtually all models is the weakness of the predicted [S II]6717, 6731 lines compared to observations. Models with densities in the 10^2- to 10^3-cm^{-3} range have [S II]6717+6731/Hα from 0.3 to 0.6 for log U between -3 and -3.5, while objects are known to have values from 0.3 to 1.6 for the same line ratio (Veilleux & Osterbrock 1987). This can be partially solved by introducing a low volume filling factor, without significant enhancement or destruction of other lines – except for the fact that the use of a low filling factor is essentially equivalent to lowering the value of the ionization parameter (Binette *et al.* 1988). The use of a filling factor, however, is essentially a mathematical trick which allows one to get extended ionized regions by artificially decreasing the densities, and should be discouraged. This is the same problem faced by Storchi Bergmann & Pastoriza's (1991) power-law models. They had to invoke sulphur overabundances to model the strong [S II] 6717+6731/Hα nuclei. However, the disagreement between the calculated and observed ratios could possibly be due to a lack of atomic data and not to the S abundance. In fact, unlike for other elements, no values for the dielectronic recombination coefficient at low temperatures are available for S ions. This mechanism could dominate both the radiative recombination and the recombining charge-transfer processes, leading to higher fractional abundances of the lower ionization states of S and to an increase of the [S II] line intensities. For all these reasons, we did not attempt any detailed modelling.

4.3 Abundances

A general conclusion drawn from the study of these and several other diagrams is that our models do work well for a good fraction of observed nuclei, although the areas occupied by Seyfert 2s and LINERs in diagnostic diagrams are not completely covered. This is clearly observed in Fig. 4 where no models reproduce [N II]/H$\alpha > 1$, a remarkable feature of many real objects, particularly LINERs. We can see no alternative, within the context of pure photoionization calculations, other than a nitrogen overabundance to explain such cases. The $n = 10^4$ cm^{-3} models with [N/H]=2 and 5 [N/H]$_\odot$ do show much improvement over any other model – integrated fluxes would obviously follow this single-density trend. Nitrogen overabundances have already been suggested by Binette (1985) and more recently by Storchi Bergmann & Pastoriza (1989, 1991). Oxygen being by far the major coolant, overabundances of nitrogen leave the ionization structure essentially unchanged, while strongly enhancing its own emission lines. In the next section we will consider the possibility that this chemical 'anomaly' may be the consequence of WR/warmers winds' dissemination on the cloudy nuclear medium.

Calculations with $Z = 0.5$ and $2\,Z_\odot$ can reproduce some AGN spectral features, but are generally less efficient regarding the coverage of AGN areas than 1-$Z_\odot$ models. Fig. 6, however, shows that $0.5\,Z_\odot$ gives the best coverage of active objects in the [O III]5007/Hβ–[O II]3727/[O III]5007 diagram. This higher excitation of 'blue' lines can readily be interpreted as due to the higher T_e in metal-poor clouds (see above). The remarkably weak [O II] of 2-$Z_\odot$ models can be understood by the inverse reasoning, lower electronic temperatures resulting in weaker [O II] emission. On the other hand, 0.5-$Z_\odot$ models result in a very narrow strip in the [O III]5007/Hβ–[O I]6300/[O III]5007 plane, whereas $2\,Z_\odot$ covers a big fraction of observational points. As a whole, only 1-$Z_\odot$ models work consistently well on diagnostic diagrams. The 0.1- and 3-$Z_\odot$ models could not fit classical AGN line ratios at all. Some low-Z models, however, could well correspond to some H II galaxies (see below). From the point of view of photoionization alone, we conclude that the 'optimum' metallicity for warmers–AGN models ranges between 0.5 and $2\,Z_\odot$, with $Z_\odot$ being strongly favoured. We also point out that although integrated models have frequently been seen as a solution to the AGN metallicity problem (Péquignot 1984; Veilleux & Osterbrock 1987), they do not allow Z to go far from $Z_\odot$. High-metallicity photoionization models must still look for other effects to provide a better fitting of the observed line ratios.

The existence of an upper limit for Z poses an interesting problem in the context of the starburst–warmers hypothesis. Since the occurrence of such stars is expected to be favoured in high-Z ambient media, one would expect that the higher the metal content the 'more active' the nucleus. At $Z \gtrsim 2\,Z_\odot$, however, cooling from forbidden lines prevents the matching of line ratios observed in Seyfert 2s and LINERs.

Regarding the photoionization calculations, although the assumption that U is constant for all clouds (which implies $n \propto r^{-2}$) can be seen as rather restrictive, a simple inspection of single-density line ratios for different values of n and U shows that no combination of them (which would simulate the existence of clouds of different densities and excitation levels) could bring much improvement to the results presented above or change dramatically our conclusions. This brings up the question of photoionization models. As fully discussed by VAG and Viegas Aldrovandi & Gruenwald (1990), photoionization models with power-law or blackbody ionizing radiation cannot account for the spread of the observational line ratios in diagnostic diagrams. As an example, although [N II]/H$\alpha > 1$ could result from a local nitrogen enrichment, it could also be produced by the coupled effect of shock fronts or high-energy electrons related to radio emission in compact sources or jets. Unless the effect of ionization mechanisms other than photoionization is analysed and discarded, it seems reckless to derive abundances from pure photoionization models.

4.4 Warmers in H II regions?

A rather intriguing result from the $Z = 0.1\,Z_\odot$ calculations is that models with the ionizing cluster in the active phase ($3.3 < t/\mathrm{Myr} < 6$), cross zones corresponding either to transition or the H II objects on diagnostic diagrams, despite the presence of warmers and the resulting extended UV emission. Even allowing for the exaggerated number of warmers

(for they should be less than the $Z_\odot$ proportion we used) one shall conclude that a metal-poor burst of star formation generating some of these stars would certainly be observed as an H II region-like object, despite its hard ionizing spectrum! The filled stars in Figs 4–6 illustrate this point. They correspond to $U=10^{-3}$ (upper star) and $U=10^{-3.5}$ (lower star) models, both having $t=3.3$ Myr, $n=10^3$ cm^{-3} and $Z=0.1\,Z_\odot$. Even the [O I] 6300 line, the most distinguishable property to separate 'normal' from active objects (due to its sensitivity to the hardness of the ionizing continuum) lies below typical AGN values for these models (Fig. 5). The $T_{\rm eff}$-sensitive He II 4686 line, however, does separate nebulae heated by warmers from those heated by normal OB stars. Its ratio to Hβ for $t=0$ models (when only main-sequence stars are present) is always smaller than 10^{-5}, whereas in the case of the above models it is ≈ 0.08 (see also Viegas Aldrovandi 1988). Apart from the He II line, the whole optical emission-line spectrum would be of a standard H II galaxy! This is actually consistent with the analysis of Melnick & Terlevich (1987), who determined ionization temperatures (using the He II line) in excess of 100 000 K for several very metal-poor H II galaxies. The compact emission-line galaxy described by Johansson *et al.* (1990) is another example.

The fact that hard ionizing continua can produce H II region-like line ratios is not exactly a new result, since some previous power-law models show the same property [see, for instance, the diagrams in Ferland & Netzer (1983) or Veilleux & Osterbrock (1987)]. This, nevertheless, was never taken as an indication that some H II regions may be heated by sources other than classical OB stars. Our results raise the possibility that at least some H II galaxies may indeed be excited by a few warmers, which would also account for the alleged rarity of these stars.

5 CHEMICAL ENRICHMENT BY STELLAR WINDS

The MM and Maeder (1990) tables give for each star its age, current mass, rate of mass loss and surface abundances by mass (X_i) of H, He, C, N and O. These data allow us to calculate the total ejected mass of an element i of a star with initial mass M at a given age t by simply numerically integrating $X_i(M,t')\,\dot{M}(M,t')$ from $t'=0$ to t (or, alternatively, $M'X_i(M')$ from $M'=$initial to present mass at age t, which yielded better numerical results). The total mass returned of a species i to the surrounding interstellar medium (ISM) by the whole star cluster is then computed by

$$M_i(t, IMF)=\int_0^t\int_{M_{\rm low}}^{M_{\rm up}}\phi(M)\,X_i(M,t')\,\dot{M}(M,t')\,dt'\,dM. \qquad (3)$$

To calculate the relative importance of this source of ISM chemical enrichment, the system (cloud + cluster + stellar-wind ejecta) is considered to be closed, in the sense that the gaseous mass at each instant is the sum of an original mass of gas and the mass input by winds, which is a reasonable assumption for the time-scales of interest (some Myr). The evolution of the gas mass and chemical abundances is then followed by solving the standard equations for the chemical evolution of galaxies (e.g., Tinsley 1980). In the case of an instantaneous burst (at $t=0$) the solution for the gas abundance of a generic element i is

$$X_i(t)=\frac{X_i(0)\,\gamma+\mu_i^*(t,\chi)}{\gamma+\mu^*(t,\chi)}, \qquad (4)$$

where $M_{\rm T}$ is the total cluster mass and $\gamma\equiv(M_0-M_{\rm T})/M_0$, M_0 being the mass of gas before the burst; $\mu^*(t,\chi)$ and $\mu_i^*(t,\chi)$ are the total stellar ejected masses of all species and of element i, respectively, per unit $M_{\rm T}/M_\odot$, at a time t and for an IMF slope χ. Converting mass to number fractions relative to hydrogen in the above equation we get a solution for the evolution of number abundances:

$$A_i(t)=\frac{A_i(0)\,\gamma+\mu_i^*(t,\chi)/a_iX_{\rm H}(0)}{\gamma+\mu_{\rm H}^*(t,\chi)/X_{\rm H}(0)}, \qquad (5)$$

where A_i is the number abundance of element i relative to H and a_i is its mass number.

Once a slope χ and the initial abundances are chosen the above equation fully determines the chemical evolution of the cloud, except for the parameter γ. The mathematical role of γ is to quantify the proportion of the pre-existing gas relative to the returned gas; the lower γ is, the more significant will this chemical 'pollution' be, and vice versa. Its plausible range of values can be found by expressing it in terms of better understood quantities, which can be done in two ways. First, if we define $M_{\rm T}/M_0$ as the burst 'efficiency' ξ (the fraction of gas converted into stars), then $\gamma=(1/\xi)-1$. An 'efficiency' of 90 per cent yields $\gamma=0.11$, whereas $\xi=10$ per cent would result in $\gamma=9$. Another possibility is to relate γ to the fraction of ionized hydrogen at $t=0$. The mass of H^+ at each instant is simply the recombination mass, given by $Q_{\rm H}(t, IMF)=[\alpha({\rm H})/m_{\rm H}]\,n_{\rm H}M_{\rm H^+}$, where α(H) is the H recombination coefficient and $m_{\rm H}$ is the proton mass. In our notation for $Q_{\rm H}$, the amount of H^+ at $t=0$ is given by $M_{\rm H^+}(t=0)=M_{\rm T}[325\,q_{47}(t=0,\chi)/n_{\rm H}(0)]$, where q_{47} is the above defined $q_{\rm H}$ in units of 10^{47} s^{-1} (Section 3), and $n_{\rm H}(0)$ is the initial cloud hydrogen density in cm^{-3}. Since $M_0-M_{\rm T}$ is the remaining gas mass just after the burst, if we consider a fraction φ of it to be in the form of H^+ we get $\gamma=1/\varphi[325\,q_{47}(0,\chi)/n_{\rm H}(0)]$. For instance, for an initially fully ionized cloud with a density of 3000 cm^{-3} and an IMF slope of 1.35 we would have $\gamma=0.15$.

The pattern of chemical changes in the cloud is shown in Fig. 7, where we plot the evolution of number abundances of C (dotted line), N (solid line) and O (dashed line) relative to their initial values [i.e., $A_i(t)/A_i(0)$] for two different values of γ. Solar values for the initial abundances and a slope $\chi=1.35$ were used. (Helium changes, which are not plotted for the sake of clarity, are of the order of 50 per cent for $\gamma=0.1$ and 10 per cent for $\gamma=1$.) Two main features are evident in this picture. First, lower values of γ increase the pollution, as expected from equation (5). Secondly, nitrogen is the first element to become noticeably overabundant, which occurs due to the fact that WN stages precede WC and WO ones. Thus, for instance, in the $\gamma=0.1$ case, while N is enhanced by a factor of 2 at ≈ 3.3 Myr, C increases by only 1 per cent and O is 5 per cent depleted compared to their initial abundances (due to the H input by the winds, which dilutes the metal pollution). Near 4 Myr, the integrated contribution from WC and WO stars becomes very strong, especially in the form of carbon, which, being expelled in great amounts

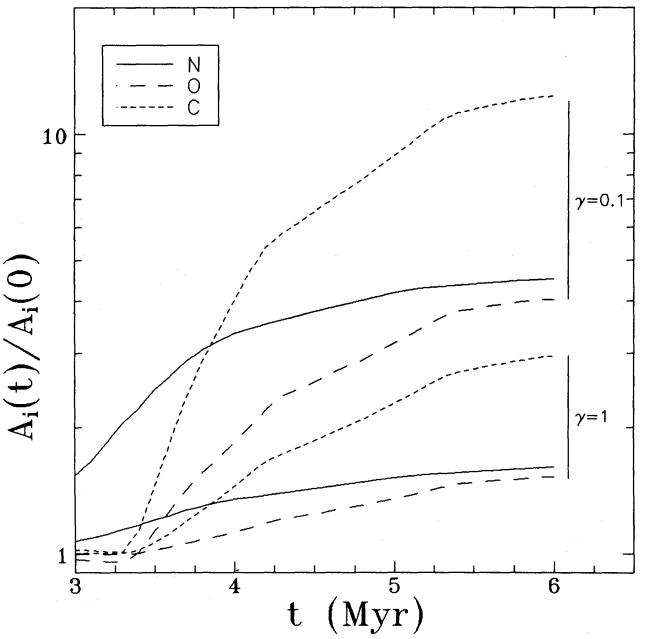

Figure 7. Evolution of the C, N and O abundances with respect to their initial values for two values of the parameter γ (see text).

during this stage, grows by a factor of 5 in about 1 Myr! Oxygen evolves more slowly, being always below nitrogen. The same description holds for the $\gamma = 1$ case, but with much smaller abundance changes. Smaller values of χ (i.e., a greater proportion of high-mass stars) result in greater variations in all species, particularly N. For example, at 3.3 Myr, while C and O would be still unchanged, N would already be 3.5 ($\gamma = 0.1$) or 1.5 ($\gamma = 1$) times enriched if χ was 0.5. At the 'onset' of WC and WO contributions, around $t = 4$ Myr, C, N and O would be about 7.2, 5.6 and 2.8 ($\gamma = 0.1$), or 2.4, 2.1 and 1.4 ($\gamma = 1$) times more abundant than initially.

Although significant quantitative differences are introduced, the generic behaviour observed in Fig. 7 is the same for the new Maeder (1990) evolutionary tracks. Because of the greater mass-loss rates, these same calculations performed with the new $Z_\odot$ and 2-$Z_\odot$ sets of tracks result in still greater wind-pollution effects. At 4 Myr, for example, the 2-$Z_\odot$ tracks yield C, N and O 13.8, 4.8 and 1.9 times greater for $\gamma = 0.1$, and 3, 1.6 and 1.1 for $\gamma = 1$, respectively (Cid Fernandes *et al.* 1991).

What can one conclude from all these pollution calculations concerning the starburst–warmers scenario for AGN? First of all, we have shown that such effects can be very significant in this picture, depending mainly on the amount of gas to be enriched (which is related to γ). Secondly, and more important, the fact that nitrogen is the first species to become overabundant may be the key to understanding the N overabundances claimed to take place in some nuclei, especially LINERs (Binette 1985; Storchi Bergmann & Pastoriza 1989, 1991). In this model, type 2 Seyferts and LINERs would behave in analogy to WR ring nebulae, where strong N pollution is observed. It is very illustrative to observe that the position of these objects on the [N II] 6583/Hα–[O III] 5007/Hβ diagram overlaps the region of AGN (Vilchez & Esteban 1991). From the point of view of photoionization models, calculations with enhanced N bring much improvement over solar-scaled models, which is clearly seen in Fig. 4. It is vital to understand that if oxygen is also enhanced by the same factor this would no longer be true, i.e., no improvement would occur to the fitting of the N lines, which is clearly seen in the 2-$Z_\odot$ models in the same figure. As discussed above, this is due to the oxygen role as the major cloud coolant. The delay between N and O enrichment observed in Fig. 7 allows us to speculate that these observed N anomalies could be interpreted in the context of wind pollution. During a period of about 1 Myr, N would be enhanced, while the low O enrichment would prevent cooling of the cloud. It must also be recalled that the wind does not mix itself instantaneously with the surrounding clouds. A typical 'diffusion' time would be something around 0.5 to 1 Myr (the time required for a 10^3-km s^{-1} wind to fill a volume of some hundreds of pc, which can be taken as a typical size for the narrow-line region). This is to say that the effective pollution time is retarded with respect to the cluster evolutionary age, which corresponds to a horizontal shift of ≈ 0.5–1 Myr in the direction of increasing time on Fig. 7. Since we expect to see emission lines only while warmers are alive to heat up the clouds, which happens only up to ≈ 6 Myr, we conclude that no matter what strong abundance anomalies are introduced during the late stages of the cluster evolution, they would not be observed! Moreover, the peak of N pollution occurs between 3.5 and 4.5 Myr (allowing for a diffusion time of 0.5 Myr), coinciding with the more luminous phase of the ionizing cluster, making the whole nucleus more easily observable. Older systems, therefore more C and O polluted, should be rarely observed due to the lower luminosity. The fact that such anomalous nitrogen abundances are more frequently reported in LINERs is consistent with the picture that these nuclei are less luminous and, consequently, have less ionized gas, which make them more susceptible to pollution effects.

The question of carbon enrichment is more difficult to assess because very little is known about this element (whose most intense lines are in the UV) in narrow-line AGN. In any case, from our results we expect some N-rich nuclei to be also C rich. The possibility raised above that nitrogen anomalies in LINERs could be understood in this wind-pollution picture is of course of great interest to the study of these objects, and will be better explored in a forthcoming work.

6 CONCLUSIONS

We have reviewed the starburst–warmers scenario for Seyfert 2s and LINERs and confirmed the Terlevich & Melnick result that warmers may indeed power the narrow-line spectrum in these nuclei. The most controversial assumption of the model is the very existence of such very hot stars. This may still be regarded as an open question, but the current observational knowledge about these stars reviewed above qualifies warmers at least as a good working hypothesis.

Our greater coverage of the parameter space – integrated line fluxes were calculated, several metallicities were considered, etc. – allowed us a wider perspective of the applicability of this model. The result of this inspection is that we found warmer-heated emission nebulae to resemble a good fraction of observed AGN line ratios, but we were unable to span completely the AGN areas on diagnostic diagrams, a

difficulty also faced by other photoionization models. As far as optical line ratios are concerned, warmers work as well as 'non-thermal' ionizing continua. Regarding metallicities, the starburst–warmers model proved not to work well for Z far from $Z_\odot$. Two mechanisms compete in defining the best metallicity. On the one hand, higher Z favours the occurrence of WR/warmer stages in the evolution of massive stars, so we expect metal-rich nuclei to go through AGN phases, whereas H II galaxies should be the case for metal-poor objects. We have also shown that even when warmers occur in metal-poor systems the resulting line ratios would not correspond to AGN, but to H II galaxies, in agreement with observations. On the other hand, the strong sensitivity of the nebular electron temperature to its metal content (due to the effectiveness of cooling from forbidden lines) imposes a limit of around $2\,Z_\odot$ for the nebula to emit as an AGN.

Our study of the effects of chemical enrichment of AGN clouds by the strongly processed stellar winds of WR/warmers turned out to explain the frequently suggested nitrogen overabundance of active nuclei in a very natural way.

Further improvements of the model should consider the effects of stellar winds and of supernovae with warmer progenitors. Better model atmospheres for warmers are also desirable. Also, the claims by Terlevich and collaborators that the type II supernovae phase (which follows after the Seyfert 2/LINER stages) can be the key to understanding the broad lines in Seyfert 1s and QSOs should be closely investigated. The starburst versus 'monsters' controversy continues, and important progress in our understanding of the activity phenomenon may be expected from this debate.

ACKNOWLEDGMENTS

We thank Drs T. Storchi Bergmann and R. Terlevich for making available their databanks and for fruitful discussions. This work was partially supported by the Brazilian institutions CNPq and CAPES.

REFERENCES

Abbott, D. C., 1982. *Wolf-Rayet Stars: Observations, Physics, Evolution, IAU Symp. No. 99,* p. 185, eds de Loore, C. W. H. & Willis, A. J., Reidel, Dordrecht.
Armus, L., Heckman, T. M. & Miley, G., 1989. *Astrophys. J.,* **347,** 727.
Azzopardi, M., Lequeux, J. & Maeder, A., 1988. *Astr. Astrophys.,* **189,** 34.
Baldwin, J. A., Phillips, M. M. & Terlevich, R., 1981. *Publs astr. Soc. Pacif.,* **93,** 5.
Barlow, M. J. & Hummer, D. G., 1982. *Wolf-Rayet Stars: Observations, Physics, Evolution, IAU Symp. No. 99,* p. 387, eds de Loore, C. W. H. & de Willis, A. J., Reidel, Dordrecht.
Bertelli, G., Bressan, A. G. & Chiosi, C., 1984. *Astr. Astrophys.,* **130,** 279.
Binette, L., 1985. *Astr. Astrophys.,* **143,** 334.
Binette, L., Robinson, A. & Courvoisier, T. J. L., 1988. *Astr. Astrophys.,* **194,** 655.
Bonatto, C., Bica, E. & Alloin, D., 1989. *Astr. Astrophys.,* **226,** 23.
Branch, D., Nomoto, K. & Filippenko, A. V., 1991. *Comm. Astrophys.,* **15,** 221.
Campbell, A., 1988. *Astrophys. J.,* **335,** 644.
Campbell, A., 1990. *Astrophys. J.,* **362,** 100.
Castor, J. I., Abbott, D. C. & Klein, R. I., 1975. *Astrophys. J.,* **195,** 157.
Chiosi, C. & Maeder, A., 1986. *Ann. Rev. Astr. Astrophys.,* **24,** 329.
Cid Fernandes, R. & Terlevich, R., 1991. In: *Relationships Between Starburst and Active Galaxies,* ed. Filippenko, A. V., ASP Conference Series, San Francisco, in press.
Cid Fernandes, R., Dottori, H. A., Viegas, S. M. & Gruenwald, R. B., 1991. *The Stellar Populations of Galaxies, IAU Symp. No. 149,* ed. Barbuy, B., Kluwer, Dordrecht, in press.
Clegg, R. E. S. & Middlemass, D., 1987. *Mon. Not. R. astr. Soc.,* **228,** 759.
Condon, J. J., Condon, M. A., Gisler, G. & Puschell, J. J., 1982. *Astrophys. J.,* **252,** 102.
Copetti, M. V. F., Pastoriza, M. G. & Dottori, H. A., 1986. *Astr. Astrophys.,* **156,** 111.
Davidson, K. & Kinman, T. D., 1982. *Publs astr. Soc. Pacif.,* **94,** 634.
de Jager, C., Nieuwenhuijzen, H. & van der Hucht, K. A., 1988. *Astr. Astrophys. Suppl.,* **72,** 259.
de Loore, C. W. H., 1982. *Wolf-Rayet Stars: Observations, Physics, Evolution, IAU Symp. No. 99,* p. 343, eds de Loore, C. W. H. & Willis, A. J., Reidel, Dordrecht.
de Loore, C. W. H., Hellings, P. & Lamers, H., 1982. *Wolf-Rayet Stars: Observations, Physics, Evolution, IAU Symp. No. 99,* p. 53, eds de Loore, C. W. H. & Willis, A. J., Reidel, Dordrecht.
Doom, C., 1985. *Astr. Astrophys.,* **142,** 143.
Dopita, M. A., Lozinskaya, T. A., McGregor, P. J. & Rawlings, S. J., 1990. *Astrophys. J.,* **351,** 563.
Dottori, H. A. & Bica, E., 1981. *Astr. Astrophys.,* **102,** 245.
Ensman, L. M. & Woosley, S. E., 1988. *Astrophys. J.,* **333,** 754.
Evans, I. M. & Dopita, M. A., 1987. *Astrophys. J.,* **319,** 662.
Ferland, G. & Truran, J. W., 1981. *Astrophys. J.,* **244,** 1022.
Ferland, G. & Netzer, H., 1983. *Astrophys. J.,* **264,** 105.
Ferland, G. & Osterbrock, D. E., 1986. *Astrophys. J.,* **300,** 658.
Filippenko, A. V., 1989a. *Active Galactic Nuclei, IAU Symp. No. 134,* p. 495, eds Osterbrock, D. E. & Miller, J. S., Kluwer, Dordrecht.
Filippenko, A. V., 1989b. *Astr. J.,* **97,** 726.
Filippenko, A. V., 1991. *Wolf-Rayet Stars and Interrelations with Other Massive Stars in Galaxies, IAU Symp. No. 143,* p. 529, eds van der Hucht, K. & Hidayat, B., Kluwer, Dordrecht.
Filippenko, A. V. & Halpern, J. P., 1984. *Astrophys. J.,* **285,** 458.
Filippenko, A. V. & Sargent, W. L., 1988. *Astrophys. J.,* **324,** 134.
Forbes, D. A., Ward, M. J., DePoy, D. L. & Boisson, C., 1991. *Mon. Not. R. astr. Soc.,* in press.
Garnett, D. R., Kennicutt, R. C., Chu, Y.-H. & Sillman, E. D., 1991. *Astrophys. J.,* **373,** 458.
Grevesse, N. & Anders, E., 1989. *AIP Conference Proceedings 183 on Cosmic Abundances of Matter,* p. 1, ed. Waddington, C. J., AIP, New York.
Gruenwald, R. B. & Viegas-Aldrovandi, S. M., 1987. *Astr. Astrophys. Suppl.,* **70,** 143.
Gruenwald, R. B. & Viegas, S. M., 1992. *Astrophys. J. Suppl.,* in press.
Halpern, J. P. & Steiner, J. E., 1983. *Astrophys. J.,* **269,** 237.
Heckman, T. M., 1987. *Observational Evidence for Activity in Galaxies, IAU Symp. No. 121,* p. 421, eds Khachikyan, E. Ye., Fricke, K. J. & Melnick, J., Reidel, Dordrecht.
Heckman, T. M., 1991. In: *Massive Stars in Starbursts,* p. 289, eds Walborn, N. & Leitherer, C., Cambridge University Press, Cambridge.
Heckman, T. M., Armus, L. & Miley, G., 1987. *Astr. J.,* **93,** 276.
Heckman, T., Armus, L. & Miley, G., 1990. *Astrophys. J. Suppl.,* **74,** 883.
Heckman, T. M., Blitz, L., Wilson, A., Armus, L. & Miley, G., 1989. *Astrophys. J.,* **342,** 735.
Jarvis, B. J. & Melnick, J., 1991. *Astr. Astrophys.,* **244,** L1.

Johansson, L., Westerlund, B. E. & Azzopardi, M., 1990. *Astr. Astrophys.*, **229,** 83.
Kennicutt, R. C., Keel, W. C. & Blaha, C. A., 1989. *Astr. J.*, **97,** 1022.
Kinman, T. D. & Davidson, K., 1981. *Astrophys. J.*, **243,** 127.
Kudritsky, R. P., Pauldrach, A. & Puls, J., 1987. *Astr. Astrophys.*, **173,** 293.
Kurucz, R. L., 1979. *Astrophys. J. Suppl.*, **40,** 1.
Langer, N., 1989. *Astr. Astrophys.*, **210,** 93.
Langer, N., Kiriakidis, M., El Eid, M. F., Fricke, K. J. & Weiss, A., 1988. *Astr. Astrophys.*, **192,** 177.
Lawrence, A., Ward, M., Elvis, M., Fabbiano, G., Carleton, G. & Longmore, A., 1985. *Astrophys. J.*, **291,** 117.
Leitherer, C., 1988. *Astrophys. J.*, **334,** 626.
Lequeux, J., Maucherat-Joubert, M., Deharveng, J. & Kunth, D., 1981. *Astr. Astrophys.*, **103,** 305.
Maeder, A., 1990. *Astr. Astrophys. Suppl.*, **84,** 139.
Maeder, A., 1991. *Astr. Astrophys.*, **242,** 93.
Maeder, A. & Meynet, G., 1987. *Astr. Astrophys.*, **182,** 243.
Maeder, A. & Meynet, G., 1988. *Astr. Astrophys. Suppl.*, **76,** 411 (MM).
Maeder, A., Lequeux, J. & Azzopardi, M., 1980. *Astr. Astrophys.*, **90,** L17.
McCarthy, P., Heckman, T. M. & van Breugel, W., 1987. *Astr. J.*, **93,** 264.
Melnick, J., 1987. *Observational Evidence for Activity in Galaxies, IAU Symp. No. 121,* p. 545, eds Khachikyan, E. Ye., Fricke, K. J. & Melnick, J., Reidel, Dordrecht.
Melnick, J. & Terlevich, R., 1987. In: *Evolution of Galaxies, Proceedings of the 10th European Regional Astronomy Meeting of the IAU,* p. 111, ed. Palous, J., Astronomical Institute of the Czechoslovak Academy of Sciences, Prague.
Melnick, J. & Heydari-Malayeri, 1991. *Wolf-Rayet Stars and Interrelations with Other Massive Stars in Galaxies, IAU Symp. No. 143,* p. 409, eds van der Hucht, K. & Hidayat, B., Kluwer, Dordrecht.
Melnick, J., Terlevich, R. & Eggleton, P. P., 1985. *Mon. Not. R. astr. Soc.*, **216,** 255.
Norman, C. & Scoville, N., 1988. *Astrophys. J.*, **332,** 124.
Pagel, B. E. J. & Edmunds, M. G., 1981. *Ann. Rev. Astr. Astrophys.*, **19,** 77.
Pakull, M. K., 1991. *Wolf-Rayet Stars and Interrelations with Other Massive Stars in Galaxies, IAU Symp. No. 143,* p. 391, eds van der Hucht, K. & Hidayat, B., Kluwer, Dordrecht.
Pakull, M. K. & Bianchi, L., 1991. *Wolf-Rayet Stars and Interrelations with Other Massive Stars in Galaxies, IAU Symp. No. 143,* p. 260, eds van der Hucht, K. & Hidayat, B., Kluwer, Dordrecht.
Péquignot, D., 1984. *Astr. Astrophys.*, **131,** 159.
Porter, A. C. & Filippenko, A. V., 1987. *Astr. J.*, **93,** 1372.
Rees, M. J., 1984. *Ann. Rev. Astr. Astrophys.*, **22,** 471.
Rodriguez Espinosa, J., Rudy, R. & Jones, B., 1987. *Astrophys. J.*, **312,** 555.
Rosa, M. R. & Mattews, J. S., 1990. In: *Properties of Hot Luminous Stars,* p. 135, ed. Garmany, C., ASP Conference Series, San Francisco.
Salpeter, E., 1955. *Astrophys. J.*, **121,** 161.
Sanders, D. B., Soifer, B. T., Elias, J. H., Madore, B. F., Matthews, K., Neugebauer, G. & Scoville, N. Z., 1988. *Astrophys. J.*, **325,** 74.
Shields, J. C. & Filippenko, A. V., 1990. *Astr. J.*, **100,** 1034.
Smith, L. F., 1988. *Astrophys. J.*, **327,** 128.
Solomon, P. M., Radford, S. J. E. & Downes, D., 1990. *Astrophys. J. Lett.*, **348,** L53.
Sreenivasan, S. R. & Wilson, W. J., 1985. *Astrophys. J.*, **290,** 653.
Storchi Bergmann, T. & Pastoriza, M. G., 1989. *Astrophys. J.*, **347,** 195.
Storchi Bergmann, T. & Pastoriza, M. G., 1991. *Publs astr. Soc. Pacif.*, **102,** 1359.
Tanaka, S., 1966. *Publs astr. Soc. Japan,* **18,** 47.
Terlevich, R. & Melnick, J., 1985. *Mon. Not. R. astr. Soc.*, **213,** 841 (TM).
Terlevich, R., Melnick, J. & Moles, M., 1987. *Observational Evidence for Activity in Galaxies, IAU Symp. No. 121,* p. 499, eds Khachikyan, E. Ye., Fricke, K. J. & Melnick, J., Reidel, Dordrecht.
Terlevich, E., Díaz, A. I. & Terlevich, R., 1990. *Mon. Not. R. astr. Soc.*, **242,** 271.
Terlevich, R., Tenorio-Tagle, G., Franco, J. & Melnick, J., 1991a. *Mon. Not. R. astr. Soc.*, in press.
Terlevich, R., Melnick, J., Masegosa, J., Moles, M. & Copetti, M. V. F., 1991b. *Astr. Astrophys. Suppl.*, **91,** 285.
Tinsley, B., 1980. *Fundam. Cosmic Phys.*, **5,** 287.
Veilleux, S. & Osterbrock, D., 1987. *Astrophys. J. Suppl.*, **463,** 295.
Viegas Aldrovandi, S. M., 1988. *Astrophys. J. Lett.*, **330,** L9.
Viegas Aldrovandi, S. M. & Gruenwald, R. B., 1988. *Astrophys. J.*, **324,** 683 (VAG).
Viegas Aldrovandi, S. M. & Contini, M., 1989. *Astrophys. J.*, **339,** 689.
Viegas Aldrovandi, S. M. & Gruenwald, R. B., 1990. *Astrophys. J.*, **360,** 474.
Vilchez, J. P. & Esteban, C., 1991. *Wolf-Rayet Stars and Interrelations with Other Massive Stars in Galaxies, IAU Symp. No. 143,* p. 379, eds van der Hucht, K. & Hidayat, B., Kluwer, Dordrecht.
Weedman, D. W., 1983. *Astrophys. J.*, **266,** 479.
Wesemael, F., 1981. *Astrophys. J. Suppl.*, **45,** 177.